Liquid metal-based plasmonics

Jinqi Wang,[1] Shuchang Liu,[2] Z. Valy Vardeny,[1] and Ajay Nahata[2*]

[1]*Department of Physics, University of Utah, Salt Lake City, Utah, 84112, USA*
[2]*Department of Electrical and Computer Engineering, University of Utah, Salt Lake City, Utah 84112, USA*
[*]*nahata@ece.utah.edu*

Abstract: We demonstrate that liquid metals support surface plasmon-polaritons (SPPs) at terahertz (THz) frequencies, and can thus serve as an attractive material system for a wide variety of plasmonic and metamaterial applications. We use eutectic gallium indium (EGaIn) as the liquid metal injected into a polydimethylsiloxane (PDMS) mold fabricated by soft lithography techniques. Using this approach, we observe enhanced THz transmission through a periodic array of subwavelength apertures. Despite of the fact that the DC conductivity of EGaIn is an order of magnitude smaller than many conventional metals, we clearly observe well-defined transmission resonances. This represents a first step in developing reconfigurable and tunable plasmonic devices that build upon well-developed microfluidic capabilities.

OCIS codes: (050.1220) Apertures; (240.6680) Surface plasmons; (260.3090) Infrared, far; (160.3900) Metals.

References and links

1. W. L. Barnes, A. Dereux, and T. W. Ebbesen, "Surface plasmon subwavelength optics," Nature **424**(6950), 824–830 (2003).
2. M. A. Ordal, L. L. Long, R. J. Bell, S. E. Bell, R. R. Bell, R. W. Alexander, Jr., and C. A. Ward, "Optical properties of the metals Al, Co, Cu, Au, Fe, Pb, Ni, Pd, Pt, Ag, Ti, and W in the infrared and far infrared," Appl. Opt. **22**(7), 1099–1119 (1983).
3. J. Gómez Rivas, C. Schotsch, P. H. Bolivar, and H. Kurz, "Enhanced transmission of THz radiation through subwavelength holes," Phys. Rev. B **68**(20), 201306 (2003).
4. T. Matsui, Z. V. Vardeny, A. Agrawal, A. Nahata, and R. Menon, "Resonantly-enhanced transmission through a periodic array of subwavelength apertures in heavily-doped conducting polymer films," Appl. Phys. Lett. **88**(7), 071101 (2006).
5. L. Ju, B. Geng, J. Horng, C. Girit, M. C. Martin, Z. Hao, H. A. Bechtel, X. Liang, A. Zettl, Y. R. Shen, and F. Wang, "Graphene plasmonics for tunable terahertz metamaterials," Nat. Nanotechnol. **6**(10), 630–634 (2011).
6. J. G. Rivas, P. H. Bolivar, and H. Kurz, "Thermal switching of the enhanced transmission of terahertz radiation through subwavelength apertures," Opt. Lett. **29**(14), 1680–1682 (2004).
7. D. C. Duffy, J. C. McDonald, O. J. A. Schueller, and G. M. Whitesides, "Rapid prototyping of microfluidic systems in poly(dimethylsiloxane)," Anal. Chem. **70**(23), 4974–4984 (1998).
8. B.-H. Jo, L. M. Van Lerberghe, K. M. Motsegood, and D. J. Beebe, "Three-dimensional micro-channel fabrication in polydimethylsiloxane(PDMS) elastomer," J. Microelectromech. Syst. **9**(1), 76–81 (2000).
9. M. D. Dickey, R. C. Chiechi, R. J. Larsen, E. A. Weiss, D. A. Weitz, and G. M. Whitesides, "Eutectic Gallium-Indium (EGaIn): A liquid metal alloy for the formation of stable structures in microchannels at room temperature," Adv. Funct. Mater. **18**(7), 1097–1104 (2008).
10. J.-H. So, J. Thelen, A. Qusba, G. J. Hayes, G. Lazzi, and M. D. Dickey, "Reversibly deformable and mechanically tunable fluidic antennas," Adv. Funct. Mater. **19**(22), 3632–3637 (2009).
11. T. W. Ebbesen, H. J. Lezec, H. F. Ghaemi, T. Thio, and P. A. Wolff, "Extraordinary optical transmission through sub-wavelength hole arrays," Nature **391**(6668), 667–669 (1998).
12. H. Cao and A. Nahata, "Resonantly enhanced transmission of terahertz radiation through a periodic array of subwavelength apertures," Opt. Express **12**(6), 1004–1010 (2004).
13. D. Grischkowsky, S. Keiding, M. van Exter, and C. Fattinger, "Far-infrared time-domain spectroscopy with terahertz beams of dielectrics and semiconductors," J. Opt. Soc. Am. B **7**(10), 2006–2015 (1990).
14. F. Miyamaru and M. Hangyo, "Finite size effect of transmission property for metal hole arrays in subterahertz region," Appl. Phys. Lett. **84**(15), 2742–2744 (2004).
15. H. Yasuda and I. Hosako, "Measurement of terahertz refractive index of metal with terahertz time-domain spectroscopy," Jpn. J. Appl. Phys. **47**(3), 1632–1634 (2008).
16. M. A. Ordal, R. J. Bell, R. W. Alexander, Jr., L. L. Long, and M. R. Querry, "Optical properties of Au, Ni, and Pb at submillimeter wavelengths," Appl. Opt. **26**(4), 744–752 (1987).

#159110 - $15.00 USD Received 2 Dec 2011; revised 3 Jan 2012; accepted 10 Jan 2012; published 18 Jan 2012

17. A. Podzorov and G. Gallot, "Low-loss polymers for terahertz applications," Appl. Opt. **47**(18), 3254–3257 (2008).
18. A. Agrawal, Z. V. Vardeny, and A. Nahata, "Engineering the dielectric function of plasmonic lattices," Opt. Express **16**(13), 9601–9613 (2008).
19. T. Matsui, A. Agrawal, A. Nahata, and Z. V. Vardeny, "Transmission resonances through aperiodic arrays of subwavelength apertures," Nature **446**(7135), 517–521 (2007).
20. A. Krishnan, T. Thio, T. J. Kim, H. J. Lezec, T. W. Ebbesen, P. A. Wolff, J. Pendry, L. Martin-Moreno, and F. J. Garcia-Vidal, "Evanescently coupled resonance in surface plasmon enhanced transmission," Opt. Commun. **200**(1-6), 1–7 (2001).
21. I. M. Pryce, K. Aydin, Y. A. Kelaita, R. M. Briggs, and H. A. Atwater, "Highly strained compliant optical metamaterials with large frequency tunability," Nano Lett. **10**(10), 4222–4227 (2010).
22. Y. Fainman, L. Lee, D. Psaltis, and C. Yang, *Optofluidics: Fundamentals, Devices, and Applications* (McGraw-Hill, 2010).

1. Introduction

The field of Plasmonics has grown dramatically over the last decade, because surface plasmon polaritons (SPPs) offer a number of unique capabilities for manipulating and guiding electromagnetic radiation [1]. Much of the current research effort in this field is focused on studies at visible frequencies, where gold and silver are the primary metals used. Most other metals exhibit unreasonably high propagation losses. However, as one moves to longer wavelengths, such as the terahertz (THz) and microwave spectral ranges, conventional metals, including stainless steel and aluminum, exhibit high conductivities and correspondingly low propagation losses [2]. Moreover, numerous non-metallic materials that are highly conducting have been shown to support SPP propagation, including doped semiconductors [3], conducting polymers [4], and graphene [5]. In this latter class of materials, it is possible to alter the conductivity of the medium through electrical, optical, thermal and chemical means. A change in the conductivity can alter the propagation losses associated with SPPs, which, in turn, can be used to create active THz device capabilities. However, such changes typically alter only the resonance quality [6]. It would be highly desirable to use a plasmonic medium that allows for tunable and reconfigurable device architectures.

A metallic medium that is highly flexible and can flow at room temperature, such as a liquid metal, satisfies such desires. In this approach, a liquid metal would be injected into microfluidic channels formed within a flexible mold. Such structures are commonly fabricated using soft lithography techniques with polydimethylsiloxane (PDMS) for a variety of microfluidic applications [7, 8]. An obvious liquid metal that flows readily at room temperature is mercury, Hg. However, mercury is highly toxic, and acts to minimize interfacial free energy. This latter effect can create unstable structures within microfluidic channels. Recently, Dickey and associates have shown that eutectic gallium indium (EGaIn) is an attractive alternative to Hg [9, 10]. EGaIn is composed of 78.6% Ga and 21.4% In by weight, has a melting temperature of ~15.5° C, and forms a thin oxide skin within elastomeric channels to provide mechanical stability to the fluid. In addition, EGaIn has a DC conductivity of 3.4×10^4 S/cm [9]. This value is an order of magnitude smaller than that of aluminum [2], for example, but is greater that of some of the non-metallic materials mentioned above [4].

In this work, we demonstrate the utility of liquid metals for plasmonics applications. Specifically, we show enhanced THz transmission through periodic aperture arrays [11, 12] fabricated by injection of EGaIn into an elastomeric PDMS mold. In order to explain the observations, we separately measure the complex THz refractive index of PDMS and the complex dielectric constant of EGaIn. An important aspect of the constituent materials is that they are amenable to stretching and flexing. We exploit this characteristic by measuring the transmission properties of the structures while being stretched. This represents a simple demonstration of mechanically tuning the plasmonic resonance properties of the device.

2. Experimental details

We fabricated periodic aperture arrays using PDMS, a silicone elastomer (Sylgard 184 kit, Dow Corning), and EGaIn, a liquid metal. PDMS is a commercially available elastomer that

#159110 - $15.00 USD Received 2 Dec 2011; revised 3 Jan 2012; accepted 10 Jan 2012; published 18 Jan 2012

is commonly used for microfluidic applications, and allows for fabrication using standard soft lithography processes [7, 8]. In order to create the microfluidic mold, we first fabricated 15 × 15 arrays of periodically spaced subwavelength apertures in free-standing 75μm thick stainless steel metal foils. The apertures had a diameter of 357 μm with a periodicity of 714 μm on a square lattice.

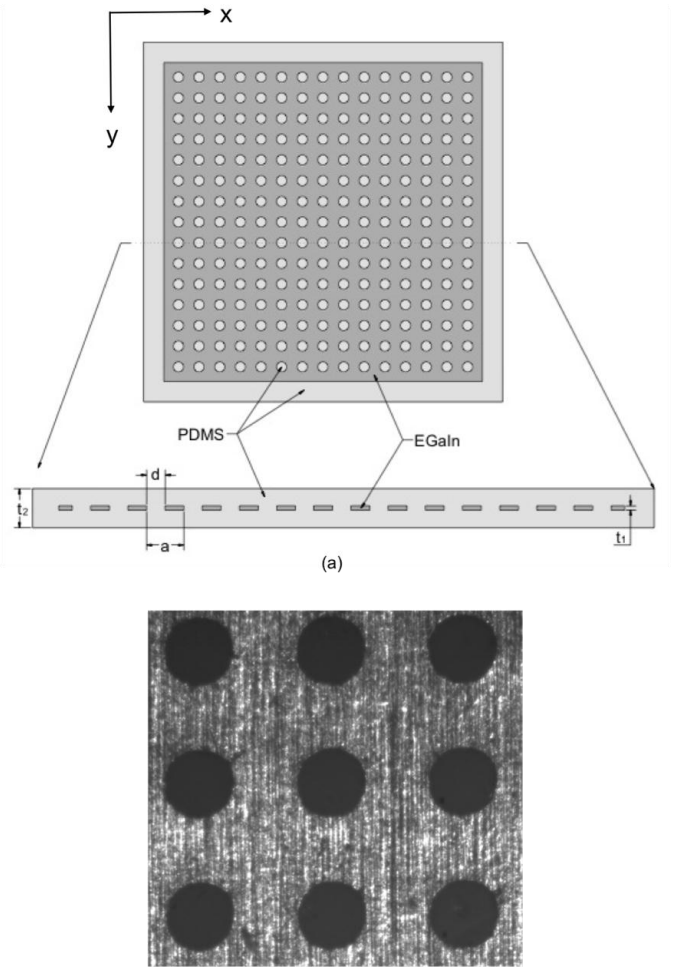

Fig. 1. (a) Schematic diagram of the top view (above) and cross-section (below) of the liquid metal aperture array encapsulated in PDMS. The aperture diameter d = 357 μm, the periodic aperture spacing a = 714 μm, the liquid metal thickness t_1 = 80 μm and total device thickness t_2 = 1 mm. (b) Photograph showing an expanded view of a portion of the array.

The perforated foils were then adhered to glass substrates using a thin (<10 μm) layer of epoxy. A PDMS pre-polymer was mixed with a curing agent using a weight ratio of 11:1, degassed, poured onto the stainless steel molds, and cured for 2 hours at 60° C. After curing, the inverse PDMS replicas were peeled off the molds and sealed with a planar section of PDMS using a high voltage corona, yielding an overall device thickness of 1 mm. Finally, we injected EGaIn into the air voids of the PDMS structures, yielding periodic arrays of subwavelength apertures based on an encapsulated liquid metal. In Fig. 1, we show a schematic diagram of the final structure with the relevant dimensions along with a micrograph

#159110 - $15.00 USD Received 2 Dec 2011; revised 3 Jan 2012; accepted 10 Jan 2012; published 18 Jan 2012

of a section of an array. For reference purposes, we also fabricated a 1 mm thick planar PDMS film.

We used THz time-domain spectroscopy (THz-TDS) to measure the optical transmission spectra, t(ν), of the electric field through the liquid metal arrays, where ν is the THz frequency [13]. In contrast to conventional optical measurements, THz-TDS allows for the direct measurement of the THz electric field, yielding both amplitude and phase information. By transforming the time-domain data to the frequency domain, we are able to determine independently both the magnitude and phase of the amplitude transmission coefficient, t(ν), using the relation

$$t(\nu) = |t(\nu)| \exp[i\varphi(\nu)] = \frac{E_{sample}(\nu)}{E_{reference}(\nu)} \quad (1)$$

In this expression, E_{sample} and $E_{reference}$ are the measured THz electric fields with either the sample or reference in the beam path, respectively, and |t(ν)| and φ(ν) are the magnitude and phase of the amplitude transmission coefficient, respectively.

Each array was mounted on a metal frame in which the opening size exposed only the metallic portion of the liquid metal array. The framed sample was placed in the path of the collimated THz beam, between a pair of off-axis paraboloidal mirrors that were used to collect, collimate and refocus the THz radiation from the emitter to the detector. The 1/e THz beam diameter was slightly larger than the aperture opening in the metal frame, thus edge effects due to the finite size of the array sample may play a role in the resulting transmission spectra [14]. In each case, the incident THz radiation was polarized parallel to a major axis of the array. Two separate reference transmission spectra were measured: one with a blank metal frame (air reference), and the other with the 1 mm thick planar PDMS film in the frame (PDMS reference). The latter reference eliminates the effect of THz absorption in PDMS.

Finally, we also measured the THz dielectric properties of EGaIn. The liquid metal is completely opaque and highly reflective at visible frequencies using a thin film that is ~2 μm thick. For this thickness, there is also no THz transmission through the liquid metal film. While it is possible to create thinner films using evaporation or sputtering techniques, the resulting film may not have the same composition as the starting metal and the composition is sensitive to the deposition conditions. Therefore, we performed THz TDS using s-polarized THz radiation in a reflection geometry to examine the properties of the liquid metal. To do so, we deposited a 2 μm thick Au film on half of a smooth metallic substrate and spread a 2 μm thick EGaIn layer on the other half. Based on the DC conductivity of EGaIn, this thickness is greater than 2 skin depths above 50 GHz. Identical results were obtained using thicker EGaIn thicknesses.

3. Experimental results and discussion

We begin by characterizing the complex dielectric properties of EGaIn, since this is necessary to demonstrate that it is capable of supporting SPPs. As noted above, we measured the reflected THz spectra from both the Au surface, which was used as the reference, and the EGaIn surface. Experimentally, we found that the amplitude reflectivity from EGaIn was ~85% that of Au over the measured spectral range. In extracting the properties of EGaIn, we used measured dielectric properties of Au [15, 16], rather than simply assuming that it behaves as a perfect reflector. In Fig. 2, we show the measured values of the real and imaginary components of the dielectric constant of EGaIn between 0.1 – 0.5 THz, clearly demonstrating that it is metallic over the measured spectral range. Given the relatively small variation in the dielectric properties, however, it is not possible to find a unique fit for the data to a Drude type function. As mentioned earlier, the reflective nature of EGaIn at visible frequencies suggests that it may exhibit metallic properties over a broader spectral range.

#159110 - $15.00 USD Received 2 Dec 2011; revised 3 Jan 2012; accepted 10 Jan 2012; published 18 Jan 2012

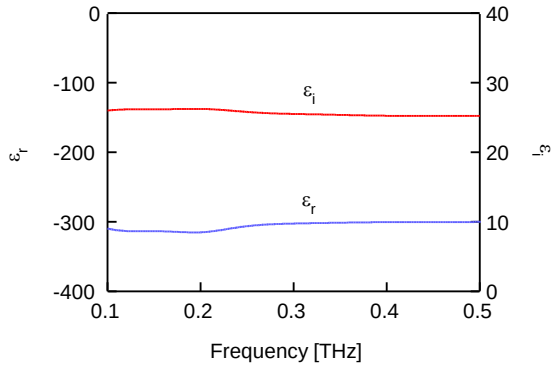

Fig. 2. Measured complex dielectric constant of EGaIn.

Next, we measured the refractive index properties of PDMS, since this parameter is important in understanding the transmission spectra of the aperture arrays. In Fig. 3, we show the measured values of the real and imaginary components of the refractive index. The real component of the THz refractive index in the spectral range of 0.1 – 0.5 THz is relatively constant, and has a value of ~1.57. The corresponding imaginary component is also largely frequency independent over that frequency range, and has a value of ~0.04. Using this value of n_i, we can readily compute the frequency dependent absorption coefficient, $\alpha(\nu) = 2\pi\nu n_i/c$ for the THz electric field, where the electric field decay is given by $\exp[-\alpha(\nu)d]$ and c is the speed of light in vacuum. Across the frequency range of interest, $\alpha \approx 0.25$ mm^{-1}, which corresponds to ~77% transmission through a 1 mm thick PDMS film. It is worth noting that the refractive index values that we find for PDMS differs significantly from published values across this same frequency range [17]. The source of this discrepancy is not clear at present, but may arise from a difference in the measured PDMS constituent mixture. As we demonstrate below, the refractive index values found here, both real and imaginary, are consistent with our aperture array transmission measurements.

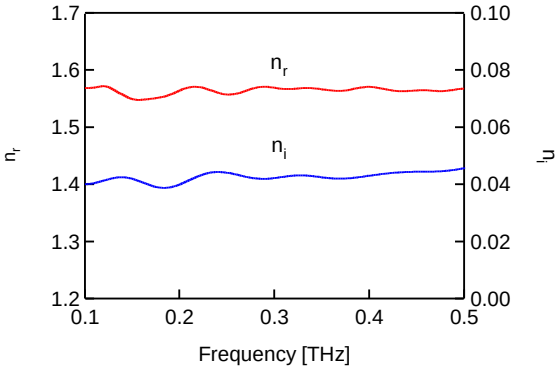

Fig. 3. Measured complex refractive index of the PDMS used in the experiment. The PDMS pre-polymer and curing agent were mixed using a weight of ratio of 11:1.

We now move to the liquid metal aperture array transmission properties. In Fig. 4(a), we show the measured transmission amplitude spectra for the liquid metal array using both air and a 1 mm thick PDMS film as references. Associated with each of the resonant peaks in the figure, there is an anti-resonance (AR) dip on the high frequency side of the resonance. It is the AR frequency that is important in understanding the experimental data. As we have shown previously, only the AR frequencies (rather than the resonance frequencies) remain fixed when the aperture diameter is varied [18]. Therefore, it is the AR frequencies that are the

#159110 - $15.00 USD Received 2 Dec 2011; revised 3 Jan 2012; accepted 10 Jan 2012; published 18 Jan 2012

relevant and fundamental parameters rather than the frequencies of the resonance peaks. From the transmission spectrum we obtained the two AR frequencies at ν_{AR1} = 0.27 THz and ν_{AR2} = 0.38 THz.

We have previously demonstrated that the AR frequencies can be found directly from the spatial Fourier transform of the real space aperture geometry [19]. In the case of a periodic array, the AR frequencies are given analytically by [11]

$$\nu_{AR} = \frac{c}{P\, n_{SPP}} \sqrt{i^2 + j^2}, \tag{2}$$

where

$$n_{SPP} = \left[\frac{\varepsilon_m \varepsilon_d}{\varepsilon_m + \varepsilon_d} \right]^{1/2}. \tag{3}$$

In these equations, n_{SPP} is the effective refractive index for the propagating SPP, ε_m and ε_d are the complex dielectric constants of the metal and adjacent dielectric medium, P is the aperture periodicity, c is the speed of light in vacuum, and i and j are integers that index the resonance order. Since the magnitudes of the real and imaginary components of the complex dielectric constant of metals is much larger than that of dielectrics, n_{SPP} typically takes a value very close to the refractive index of the dielectric medium (in this case, $n_{SPP} \cong n_{PDMS} \approx 1.57$). From Eq. (2) the two lowest order AR frequencies occur for i = ± 1, j = 0 (AR_1) and i = ± 1, j = ± 1 (AR_2).

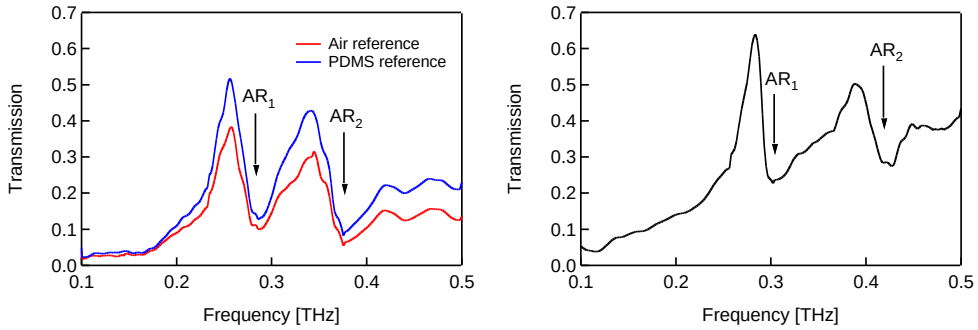

Fig. 4. THz electric field transmission spectra, t(ν) of (a) 15 × 15 liquid metal array with 357 μm diameter apertures periodically spaced by 714 μm. Air and a 1 mm thick PDMS film are used as references. (b) 15 × 15 array with 400 μm diameter apertures periodically spaced by 1 mm in a 75 μm thick free-standing stainless steel foil with air as the reference.

Using Eqs. (1) and (2), the two lowest order AR frequencies are expected to occur at ν_{AR1} = 0.27 THz and ν_{AR2} = 0.38 THz, in excellent agreement with the experimental data. As expected, the transmission spectra using air as the reference is smaller in magnitude than that when PDMS is used as the reference. In fact, the 'air reference' transmission is only ~76% that of the 'PDMS reference.' This agrees well with expectations based on the measured imaginary component of the refractive index (Fig. 2).

At this point, it is reasonable to compare the SPP enhanced transmission properties from the liquid metal hole arrays with those obtained using a more conventional metal hole array. In order to make a fair comparison, it should be noted that since the apertures in the liquid metal array are filled with the same medium that encapsulates the liquid metal on all sides (i.e. PDMS), the ratio of the effective aperture size to the effective aperture spacing remains constant and the dielectric refractive index serves to scale the effective periodicity [20]. Therefore, we also fabricated a 15 × 15 array of 400 μm diameter apertures on a square grid with an aperture spacing of 1 mm on a free standing 75 μm thick stainless steel foil, since this

#159110 - $15.00 USD Received 2 Dec 2011; revised 3 Jan 2012; accepted 10 Jan 2012; published 18 Jan 2012

geometry yields similar AR frequencies. In this case, only air was used as the reference. While the absolute transmission magnitude and the quality factor associated with the lowest order resonance for the stainless steel sample shown in Fig. 4(b), is somewhat greater than that for the liquid metal sample, it is worth reiterating that the DC conductivity of the liquid metal is smaller than that of stainless steel [2]. This is generally consistent with earlier observations of enhanced THz transmission through a periodic array of subwavelength apertures fabricated in heavily doped conducting polymers [4].

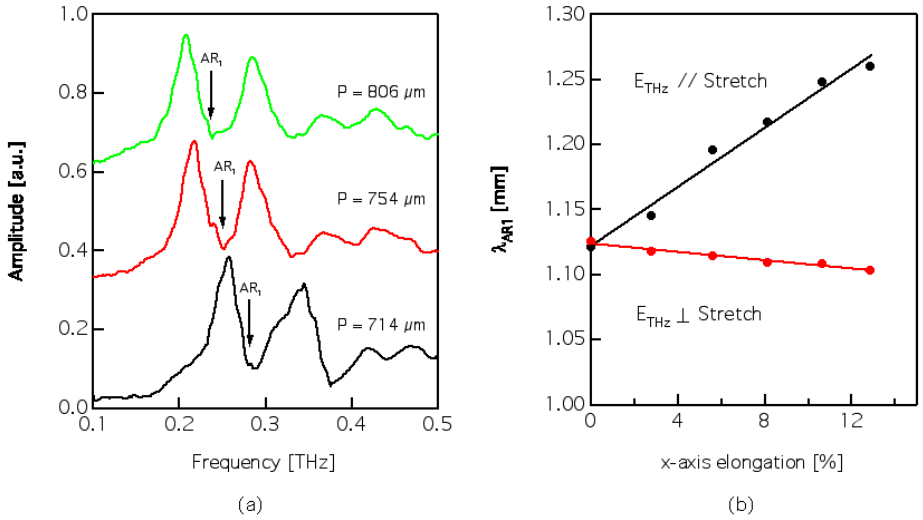

Fig. 5. Transmission properties of the 15 × 15 liquid metal array as a function of stretching the device along the x-axis (a) Measured transmission spectra for three different degrees of stretching (corresponding to different periodicities along the x-axis) with THz radiation polarized along the x-axis. The corresponding lowest order AR frequencies are marked. (b) Measured AR wavelength as a function of stretching for THz radiation polarized parallel (filled black circles) and perpendicular (filled red circles) to the stretch axis. In the absence of stretching (0% elongation), the periodicity is 714 μm along both array axes. The maximum stretched period along the x-axis of 806 μm corresponds to a ~13% elongation of the device along the stretch axis. The lines represent linear least-squares fits to the data.

In contrast to rigid substrates, such as conventional metals typically used for plasmonics applications, PDMS and liquid metals lend themselves to the idea of creating mechanically tunable and reversibly stretchable plasmonic devices. In order to demonstrate this, we measured the THz transmission properties of the 15 × 15 liquid metal array as a function of elongation along the x-axis. In Fig. 5(a), we show the measured transmission spectra of the array, with air as the reference, for three different degrees of stretching, corresponding to three different effective periodicities along the x-axis. It is apparent that ν_{AR1} does not shift in a linear manner. We therefore show the measured AR wavelength, λ_{AR1}, as a function of the fractional elongation along the x-axis in Fig. 5(b), where the unstretched film with P = 714 μm corresponds to 0% elongation and P = 806 μm corresponds to ~13% elongation. When the incident THz radiation was polarized parallel to the x-axis, we observed a linear increase in the AR wavelength with stretching. Such a variation is apparent when Eq. (2) is rewritten as

$$\lambda_{AR} = \frac{P}{\sqrt{i^2 + j^2}} n_{SPP}. \qquad (4)$$

However, when the incident THz radiation is polarized perpendicular to the stretch axis (i.e. along the y-axis), we observe a slight decrease in λ_{AR1} as the structure is stretched. The observed blue shift arises from the fact that stretching along the x-axis causes a small degree of compression along the y-axis. Over the stretching range used here, the array was reversibly deformable and the same AR wavelengths were measured upon stretching and subsequent

#159110 - $15.00 USD Received 2 Dec 2011; revised 3 Jan 2012; accepted 10 Jan 2012; published 18 Jan 2012

contraction back to the original position. Further stretching caused a nonlinear change in the measured AR wavelength. We note that analogous tuning has been demonstrated using gold-based split ring resonators fabricated on a thick PDMS substrate [21].

4. Conclusion

In conclusion, we have presented the first experimental demonstration of plasmonics using liquid metals. To do so, we fabricated periodic arrays of subwavelength aperture arrays with EGaIn injected into an elastomeric PDMS mold, and measured the enhanced THz transmission properties of static arrays as well as arrays that were mechanically stretched. The latter measurements show the capability for mechanically tuned plasmonic devices, and may allow for more complex three-dimensional plasmonic architectures. Since EGaIn flows at room temperature, we expect that many of the sophisticated technologies developed for microfluidics and optofluidics [22] may be used to develop a broad range of *active plasmonics* capabilities. While the specific demonstration here relates to plasmonics, this approach can also be extended to develop active metamaterial devices. Although the measurements discussed here were performed at THz frequencies, further studies of the dielectric properties of EGaIn may show that it can be used for plasmonic and metamaterial applications over a much broader spectral range.

Acknowledgments

This work was supported through the National Science Foundation MRSEC program under grant #DMR-1121252. We also acknowledge funding from the University of Utah Open Access Publishing Fund.

#159110 - $15.00 USD Received 2 Dec 2011; revised 3 Jan 2012; accepted 10 Jan 2012; published 18 Jan 2012